ACCEPTED MANUSCRIPT available at https://iopscience.iop.org/article/10.1088/1741-4326/abfd71
DOI 10.1088/1741-4326/abfd71

Nuclear design and assessments of HELIAS-type stellarator with DCLL BB: adaptation from DEMO tokamak reactor

Iole Palermo[1], Felix Warmer[2], André Häußler[3]

[1] CIEMAT, Fusion Technology Division, Avda. Complutense 40, 28040-Madrid, SPAIN
[2] Max Planck Institute for Plasma Physics (IPP), Wendelsteinstr. 1, 17491 Greifswald, Germany
[3]Karlsruhe Institute of Technology (KIT), Hermann-von-Helmholtz-Platz 1, 76344 Eggenstein-Leopoldshafen, Germany

E-mail: iole.palermo@ciemat.es

Received xxxxxx
Accepted for publication xxxxxx
Published xxxxxx

Abstract

As possible long-term alternative to a tokamak fusion power plant, the stellarator concept offers salient physics features (no external current drive, no risk of plasma disruptions, low recirculating power, among others) which could be offset by the more complex configurations and challenging maintenance schemes. Very little in the way of conceptual design studies has been performed compared to tokamaks and enhancement of engineering aspects should follow. With the recent start of operation of Wendelstein 7-X, the Helical-Axis Advanced Stellarator (HELIAS) line has raised again interest among the scientific and technologic EUROfusion Programme. The main aim at present is showing that stellarators (particularly helical axis stellarators) are viable as potential fusion reactors. To follow on the conceptualization of a mature HELIAS power reactor, different engineering and technological aspects must be studied, improved and solved. To this end, starting from a very preliminary reactor design called "HELIAS 5-B" (5-field-period) with a fusion power of 3000 MW, a neutronic model has been developed and analysed introducing in the baseline the relevant components of Breeding Blankets (BB). The large experience achieved at CIEMAT in BB designs for DEMO tokamak has been exploited, adapting the Dual Coolant Lithium-Lead Breeding Blanket (DCLL BB) design elaborated in the frame of the WPBB Programme of EUROfusion/PPPT, to the HELIAS configuration. Preliminary neutronic assessments have been performed focusing on tritium production, power density distributions and damage/shielding responses as nuclear heating, neutron fluence, dpa and helium production. Particle transport calculations have been performed with MCNP5v1.6 Monte Carlo code.

Keywords: HELIAS, DCLL BB, MCNP, Neutronic performance

1. Introduction

On the way toward the realization of a commercial fusion power plant, following the ITER line, the DEMOnstration tokamak reactor design has centralized the most of the research and development European efforts over the last decade. However, with the recent start of operation of Wendelstein 7-X, the Helical-Axis Advanced Stellarator (HELIAS) [1] line has raised again interest among the scientific and technologic EUROfusion Programme which dedicates a mission of its own to stellarator research in the Fusion Roadmap [2]. The stellarator is a possible long-term alternative to a tokamak fusion power plant. In the short-term, the main priority is the scientific exploitation of Wendelstein 7-X. However, preparatory pre-concept design studies can be performed sooner, using the evolving experience from ITER and the tokamak DEMO work. The ambitious programmatic strategy to high-performance, steady-state operation will include a critical assessment of optimised stellarators as an alternative fusion power plant concept. Therefore, a first optimisation of the power plant configuration of the HELIAS line has started [1].

Substantial progress has been made in understanding stellarator plasmas and important advancements have been already obtained on the physics aspects. From the technology research side, the main aim at present is showing that stellarators (particularly those of the HELIAS line) are viable contenders for a potential fusion power reactor. To follow on the conceptualization of a mature HELIAS reactor, different engineering and technological aspects have to be studied, improved and solved.

A very preliminary design (Figure 1) called “HELIAS 5-B” (5-field-period), with a fusion power of 3000 MW [3], which is a simple linear extrapolation of Wendelstein 7-X, has been developed. Although in the future, different stellarator designs could be also considered.

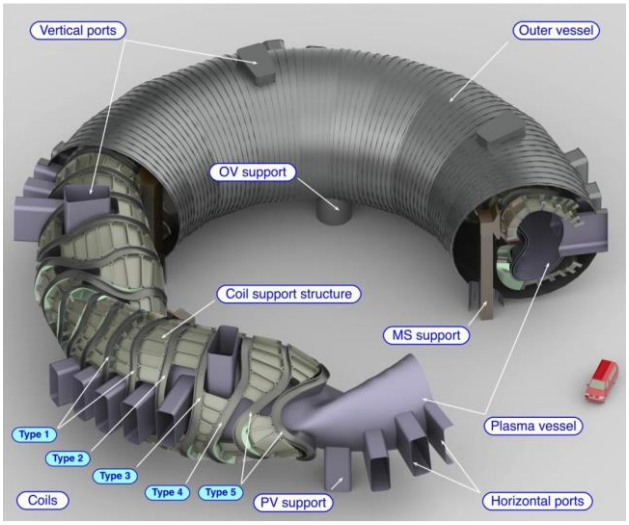

Figure 1: 3-D view of the Helias-5B power reactor [3]

Based upon this, a simplified neutronic model has been constructed [4] introducing in the baseline CAD model the relevant components of Breeding Blankets (BB) inside a simplistic model of Vacuum Vessel (VV) and superconductive non-planar shaped field Coils.

In fact, the future stellarator reactor must be equipped with a breeding blanket system in order to guarantee the fuel (tritium) self-sufficiency of the reactor. The neutrons coming from the fusion plasma of large machines, like HELIAS, could severely affect the stability and the lifetime of the components that constitute the reactor. Nevertheless, neutrons are fundamental to allow the reactor to reach the tritium self-sufficiency and to generate and extract enough nuclear power. This means that in the nuclear design of this kind of facilities it is essential to achieve and keep the delicate balance among fuel sustainability and power efficiency vs. radiation shielding.

Thus preliminary neutronic assessments have been performed focusing on: neutron wall loading (NWL), tritium production, power density and shielding responses as nuclear heating, neutron fluence, displacement per atom (dpa) and helium production.

The specific challenges of a stellarator, that are different from the ones that presents a tokamak, have been addressed starting with the crucial differences in the neutronic approach both for modelling than for assessments. In fact, due to the more complicated nature of stellarator neutronics analyses, simplified approaches to fusion neutronics, already developed for tokamaks, have been even more important for designing a conceptual stellarator reactor. Furthermore, the need for 3D neutron distributions - instead of tokamak 2D analyses - to adequately represent the variation of the neutronic responses also in the toroidal direction in complex geometries as the stellarator one is highlighted.

It has to be emphasized that differently from neutronics for tokamaks, the state of the art of the neutronics for stellarators is quite limited and still primitive. Preliminary developments, assessments and 2D neutronics results have been found in literature [5][6][7] and some 3D new approaches have been considered only recently [8][9] [10][11][12].

Despite the three-dimensional freedom of stellarators, only a limited number of conceptual stellarator reactor designs are under assessments in the world, and as a consequence there is not an established procedure for the development of 3D neutronic designs, a standard approach for 3D neutronic assessments and a common methodology for visualization of such complex results.

Therefore, unique developments and results are described in this paper.

2. DCLL BB adaptation from DEMO to HELIAS

Following the previous considerations, a collaboration within IPP, CIEMAT and KIT has recently started for the assessment of stellarator-specific aspects of the blanket design. While KIT dedicated many efforts to the design and analyses of the Helium Cooled Pebble Bed (HCPB) BB concept [9][10][11] for HELIAS, CIEMAT has focuses in the development and preparation of a Dual coolant Lithium-Lead Breeding Blanket (DCLL BB) model within the HELIAS geometry. The large experience achieved at CIEMAT in BB designs for DEMO tokamak has been exploited, adapting the DCLL BB design [13][14], which was elaborated in the frame of the PPPT EUROfusion Programme for DEMO, to the HELIAS configuration. Ultimately this work shall lead to a detailed knowledge basis of the neutronics properties in next-step HELIAS devices and should consequently push the development of a stellarator-specific breeder blanket. The activities performed have focused on a preliminary adaptation of the DCLL BB modules to the stellarator structure giving sequential approximations for preliminary assessments of the main nuclear responses.

The DCLL HELIAS neutronic model has been developed through the MCAM (Monte Carlo Modeling Interface Program) tool SuperMC_MCAM 5.2 Professional Version [15], an integrated interface program between commercial CAD software (here CATIAv5 [16]) and Monte Carlo radiation transport simulation codes. Using the MCAM tools, the simplification of the CAD model has been pursued and it has been adapted to the MCNP code [17] in terms of spline approximation to faceted surfaces, void creation and decomposition, gluing of pieces of the same component, and splitting of others. In fact, one of the main difficulties in the realization of a neutronic model of a Stellarator suitable for MCNP resides in the fact that the apparently simple structures that conform the generic HELIAS baseline CAD model are very complex in term of kind of surfaces which constitute them. Only splines are used in the CAD model and no approximation to surfaces that stand on first or second degree equations are employed, as the MCNP code requires. Having identified the CAD modelling as a bottleneck, the future work will also focus on developing new, more compatible type of CAD models.

2.1 DEMO DCLL BB main features

During the two periods 2014-2018 and 2019-2020, CIEMAT led the development of the EUROfusion BB DCLL design for DEMO tokamak, under the WPBB and WPENR PPPT Programmes, respectively. The DCLL concept considered in the first period was a modular BB design in which a common Back Supporting Structure (BSS) is connecting a different number of modules inside a poloidal torus segment to speed-up and simplifies the injection of the fluids and the Remote Handling (RH) operations. This configuration is known as Multi-Module Segment (MMS). The evolution of such design and their neutronic analyses is widely described in [18][20][21][22][18][23][24][25].

Most recently, under WPENR, another configuration called single module segment (SMS), also defined as "banana-shaped" blanket, has been studied for the DCLL [27] opening a wide range of segmentation possibilities especially interesting for the complex and varying 3D shape of HELIAS.

The breeder and neutron multiplier in a DCLL is PbLi eutectic (with Li-6 enrichment at 90%), the coolants are both the PbLi cooling itself and the Helium for the cooling of the First Wall (FW) and the stiffening grid. The liquid metal flows at high velocity to extract most of the reactor power. The high velocity in a strong magnetic field could provoke huge MHD (magneto-hydro-dynamic) effect (pressure drop). This can be corrected through a special component called Flow Channel Insert (FCI) which isolate electrically (and thermally) the PbLi from the magnetic field.

One of the last MMS DEMO DCLL BB model, called v3.1 (Figure 2) [13][14] developed for the WPBB DEMO programme and based on the plasma parameters of DEMO2015 [28][29] (i.e. 2037 MW and pulsed scenario[30]), has been preliminarily adapted to the complex 3D geometry of HELIAS.

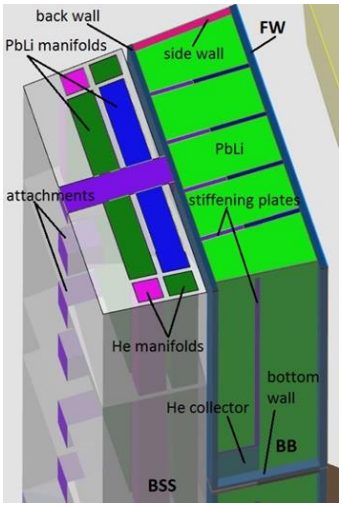

Figure 2. IB BB and BSS of the DCLL DEMO [13]

2.2. DCLL advantages/disadvantages

The main advantages of this kind of liquid breeding blanket in comparison with the other 3 concepts (Helium Cooled Pebble Bed (HCPB), Helium Cooled Lithium Lead (HCLL) and Water Cooled Lithium Lead (WCLL)) studied among the EUROfusion Programme [31] are:

- Wider design margins due to the double cooling system
- Lower tritium inventory (and it can be avoided HTO formation)
- No safety issue related to water cooling

• No safety issue related to Be multiplier
• Well suited for presently available nuclear materials
• Well suited for Eurofer (upper temperature limited)
• Potential for high-temperature and higher plant efficiency

All these advantages made the DCLL BB concept probably one of the concepts with highest long term potential of improvement and of the most adaptable to the physic and technology challenges which poses the stellarator configuration.

The main concerns regarding the DCLL are:

• Not tested in ITER (Test Blanket Module (TBM))
• Design difficulties linked to relatively high PbLi velocity
• MHD problems (FCI under development)
• Corrosion problems

The last 2 issues also could undermine the HCLL and WCLL concepts based on the same metal liquid than the DCLL.

2.3 Considerations on the viability of a DCLL blanket for HELIAS and possible approach for easy fit from DEMO

Previously to the definition of a BB design for HELIAS it is very important to identify the synergies between DEMO and HELIAS research programmes (not only technological – components, materials, maintenance schemes - but also in terms of methodology, modelling, analysis tools, among others) and identify both:

• the common mainstays that can be used to exploit to the maximum the knowledge acquired in BB DEMO and
• the main discrepancies on which to act from the beginning in order to design a first scheme of blankets for stellarator (segmentation, shape of the FW and of the modules, space available for BB/BSS, use of better shields to obtain good answers in a reduced space).

To streamline the development of the BB for HELIAS 5-B, the experience and results achieved for DEMO should be exploited as much as possible. Recognizing the differences between the two machines will be essential to progress. Some of the most important points are summarized as follows:

1. Plasma volume, power and sector size parameters

The baseline for EUROfusion DEMO determined by the PROCESS system code changed several times from 2014 to 2017 [32] [28] [33]. The adopted in 2015 [28] being the baseline for the DCLL v3.1 established a modification from the previous 16 to 18 TFC and resulted in a larger and more powerful plasma (from 1400 to 2500 m^3 of volume and from 1572 to 2037 MW of fusion power).

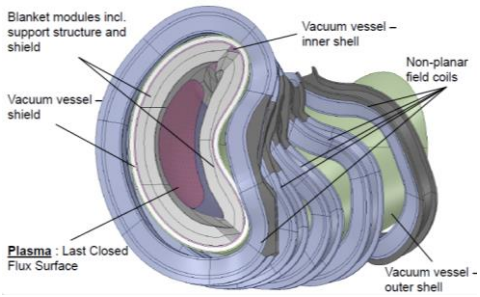

Figure 3. 36º CAD model for neutronic model development

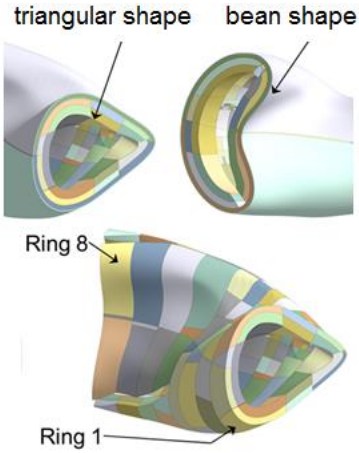

Figure 4. Shape, nomenclature and numeration of the rings which form the sector

The current baseline for HELIAS 5-B [3] has a plasma volume of 1407 m^3, 3000 MW of fusion power and 50 non-planar shaped field Coils.

A generic HELIAS CAD model [34] has been provided by KIT with the available space left for blanket (Figure 3). The model includes a half period of 36º (from 36 to 72º), since thanks to the toroidal symmetry (5 periods) inside the stellarator configuration, it allows to reproduce the full responses in the whole machine. It also means that comparing with the 11.25º sector modelled in DEMO, for a similar degree of detail the HELIAS modelling would imply a larger number of cells and surfaces in the neutronic design. The numeration of the 8 rings which conform the sector and the nomenclature for their shape can be found in Figure 4.

2. Available space for blankets

The main radial dimensions for the BB + BSS in the DEMO are 39.8 cm + 36 cm in the IB side and 63 cm + 63.7 cm in the OB side, respectively. The current radial build for HELIAS BB components is shown in Figure 5 [35]. The radial dimensioning has a continuous variation in both the toroidal and poloidal directions. Comparing the total of 50 and 75 cm considered for the IB and OB sides of HELIAS at the equatorial plane of the Ring 8 (enlargeable 15 cm more, according to the available space between the depicted BB zone and the VV) with the higher dimensions of DEMO BB, it is clear that for the development of a BB for HELIAS, the

BB+BSS configuration should be rearranged to cope with a reduced space. Nonetheless as the general dimensions of the stellarators are very different from DEMO this not implies necessarily a negative prevision on the neutronic performances of the DCLL BB, also taking into account the very good coverage of breeding structure around the plasma (due to small divertor dimensions and no big penetrations for Neutral Beam Injectors, for example).

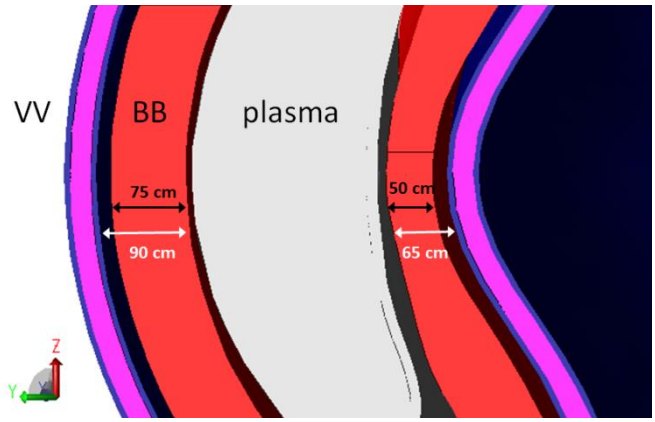

Figure 5. Space available for breeding and shielding structures vs. actual region created in CAD model.

3. Materials of reactor components

For the components of the generic DEMO the following materials are considered:

• Vacuum Vessel: 60% austenitic steel + 40% H_2O.

• Coil case: austenitic steel

• Coil winding Pack, conductor and epoxy insulator: Nb_3Sn + cryogenic steel + epoxy + Bronze + Cu + He + vacuum.

These have been also used in HELIAS.

Among the DEMO development programme it was demonstrated [36] the high impact of the divertor composition on the tritium production performance (among others) especially for no water cooled BB concepts. The current HELIAS design has 2 divertors/limiters which composition, as learnt from DEMO, will influence very much the neutron transport in the BB (due to the back-scattering inside the plasma chamber). This point should be carefully addressed, although, in the preliminary design phase, there is no divertor inside the CAD model.

4. Segmentation, gaps, distance of the FW from plasma

The segmentation has to answer the important function of simplify RH procedures, but at the same time allowing that the BB modules are as much as possible near the plasma, but without interfering with the Scrape Off Layer. The BB segmentation adopted for DEMO could be very different for HELIAS according to the specific maintenance scheme in the stellarator (location, size and number of ports). Thus, the MMS used at the beginning for DEMO designs to speed up the RH operations could vary by using different number of modules (according to the best fitting to the new plasma shape) and furthermore the SMS could be studied as option.

The gaps between modules have to allow the deformation and expansion of the modules without crashing one to each other. In DCLL DEMO gaps of 20 mm have been used both in poloidal (between modules) and in toroidal direction (between segments).

Furthermore, as learned from DEMO, will be important to know which will be the last magnetic plasma surface in case of off-normal events (if any, as so far not observed in stellarators) to design a functional FW able to withstand with the heat loads.

5. Modelling and analysis tools

Most of the tools used for DEMO neutronic modelling/analyses/representation (SuperMC_MCAM 5.2 [15], SpaceClaim [37], MCNP5v1.6 [17] and Paraview [38]) seem feasible to be used also for the assessment of the DCLL HELIAS although with the appropriate modifications of source term. The plasma neutron source was provided by KIT as a FORTRAN90 subroutine [39]. Furthermore, an improved licence of SuperMC has been required considering the higher number of cells and higher size of the sector comparing with the DEMO one, to allow the creation of the MCNP geometry input card.

3 DCLL BB HELIAS models

Before the implementation of the BB zone and the adaptation and design of the DCLL for HELIAS, the generic HELIAS CAD model has to be simplified to be used in the transport code MCNP. This code only allows geometries consisting of surfaces that can be described by 1st order equations like planes, 2nd order equations, parabola, hyperbolas and 4th order as elliptical torii. But nevertheless, almost all the surfaces of the starting HELIAS CAD model are made by splines which are not supported by the constructed solid geometry for MCNP. This fact complicated very much the preliminary phase of the geometry creation of the HELIAS generic model. Furthermore, two of the three main components of the model, the plasma and the VV, were made by very big single pieces that the MCAM code was unable to convert in an MCNP format.

Due to all these difficulties different procedures has been implemented being each new approach a consequence of the failure of previous one. They were especially time consuming and a hard manual task. Each step of the procedure has been implemented different times with different degree of accuracy up to obtain an apparently viable component convertible in MCNP format. In fact, each step has been tested by partial conversion of each developed zone to MCNP format to verify its viability. To overcome these complications, 3 different models have been finally developed, focusing on the specific analyses to be performed with each one.

The first model (Section 3.1) is the one used for the shielding responses, so centred on the analyses concerning the VV and Coil. In such model the BB zone is homogenized while the VV and Coil are included in detail in Ring 8 (see Figure 4 for location of such ring). This is due because this ring is one of the most irradiated according to the neutron wall loading, nuclear heating and neutron fluxes results described in Section 4.

The second model (Section 3.2) has a more detailed BB description, at least in part of the Ring 8 and has been used for tritium production enhanced calculations.

The third model (Section 3.3) has only the plasma, a voided BB structure and specifically created new complementary voids in between, and it has been used for the NWL calculation.

The models development is described in the following sections. Only the successful procedures are reported.

3.1 Generic DCLL HELIAS model for shielding analyses

The model includes the plasma, BB and VV as described in the following points. Furthermore, the possibility of filling the space between BB zone and VV with components representative of the BBS/manifolds has been explored, since such void space of 15 cm thickness could be unnecessary. A simplified model of the coils has been also required. Then, a CAD model of such coils has been provided by IPP [40] as essential input for the following analyses (Figure 6). The superconductive coils have been reduced to a simplistic model occupying only the most irradiated zones (Figure 7) that, according to the analyses of Section 4, are around the equatorial plane of the Ring 8, among other zones.

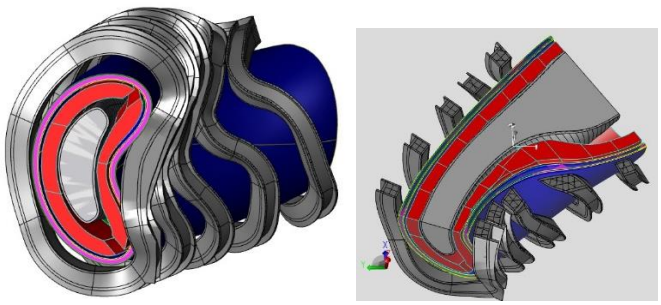

Figure 6. CAD input of the 5 Coils inside the 36º sector of HELIAS 5-B. The coils (grey) are integrated in the model composed by the VV (blue), BB (red) and plasma (white).

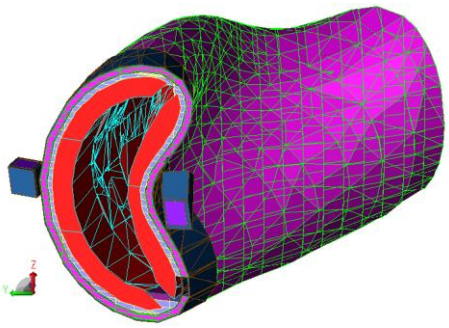

Figure 7. Neutronic model of DCLL HELIAS used for most of the neutronic analyses: simplification of the superconductive Coil (blue and violet) in smaller pieces occupying only the areas of interest for the consequent analyses; 3 layered VV for Ring 8 (blue-pink-blue), 1 massive VV layer (pink) for Rings 1-7; an intermediate shielding layer (lilac) for Ring 8; homogenized BBs (red).

1. Regarding the plasma, favourably, the plasma single cell (Figure 8, white body) was made by a combination of surfaces described by quadratic equations. For this reason, in order to simplify such a big cell, it has been simply split according to the planes X, Y and Z, in X=50, Y=5 and Z=10 sections, obtaining a total of 2496 smaller and simpler cells.

2. Concerning the BB zone, the BB CAD model consisted of 40 cells (or segments) made of splines surfaces. Such cells (Figure 8, red components) have been faceted through an automatic tool of SuperMC with an accuracy of 20 cm (see figure 8, the red smoothed region in the upper figure has been converted in pieces of a more squared-shape as in the figure below). The process allows converting the 40 cells in MCNP input format. Some reduction of the BB volume was unavoidable, but the resultant geometry was still representative of the real shape of the BB zone. The loss of breeding volume due to the faceting process is of a 2.27%. This breeder volume loss can be taken into account in the calculation of the final Tritium Breeding Ratio (TBR) adding a 2.27% as direct contribution to the initial value.

In Figure 8 it is possible to observe how the faceted process works to approximate the splines to planes, and the subdivision in little pieces to allow a good conversion to MCNP. Furthermore, taking into account possible difficulties to manufacture such a complicated BB shapes, the faceted shape could be a more realistic configuration for a future blanket.

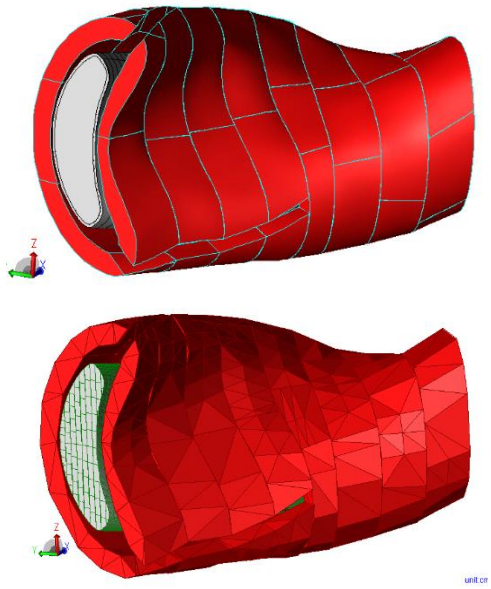

Figure 8. Breeding zone simplification through "FacetBody" tool of MCAM with 20 cm accuracy

3. Regarding the Vacuum Vessel, in the original CAD model it is represented by 3 layers: 2 external steel layers of 6 cm each one, plus an intermediate layer of 20 cm made by a mixture of water and steel. During 2018 [35] it was ruled out to simplify and convert the thin layers, since resulted impossible to faceted them, because with 20 cm accuracy the thin 6 cm layers were completely broken-down, while with 10 cm accuracy the process was eternalized probably due to lack of RAM or problems with the SuperMC license and the maximum number of cells manageable. These problems have not appeared with the new 2019 license and a new PC. So, in this second phase of the model development [41], and also in order to avoid the above mentioned outcome due to the maximum number of cells manageable by SuperMC, the 8 rings of the 36º sector has been treated with different degree of detail: Ring 8 with higher accuracy than Rings 1-7 (Figure 7 and 9). For Rings 8 the 3 VV layers have been included; the splines, have been faceted with SuperMC selecting a 10 cm accuracy. Then, the faceted layers have been split in Y=4 and Z=10 sections. For Rings 1 to 7 only 1 massive VV layer has been included; the splines, have been faceted with SuperMC selecting a 20 cm accuracy. Then, the faceted layer has been split in X=8, Y=10 and Z=4 sections.

The loss of Vacuum Vessel volume due to the faceting process is around a 3%.

Further details can be found in [41]. Some representations are given in Figure 9.

In the pictures the different components treated with different degree of accuracy are shown:

- In pink the massive Vacuum Vessel layer occupying Rings 1-7 made by a mixing composition of steel and water: SS316LN 60%; H_2O 40% - called m60
- In blue the 2 VV external layers of Ring 8, made by Austenitic Steel SS316LN – called m50
- In pink the internal layer of the VV of Ring 8 made by water and steel (m60)
- In violet the intermediate layer between BB and VV to use as shielding (a mixture of 71.84% Eurofer, 26.365% PbLi, 1.795% He –called m71 – has been used in a first attempt to reproduce the BSS of the DCLL DEMO model) only in Ring 8. For the other rings this layer is absent.
- In red, the space left for Blanket or Blanket+BSS/Shielding depending on the achieved T production capabilities. Two compositions [4] have been tested:
- 24.5% Eurofer, 70.5% PbLi, 4.4% He, 0.5% W, 0.16% Al_2O_3 – called m24
- 41.696% Eurofer, 52.485% PbLi, 5.477% He, 0.255% W, 0.087%Al_2O_3- called m41.

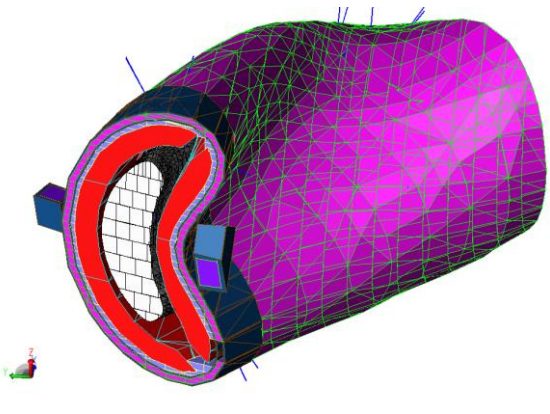

a)

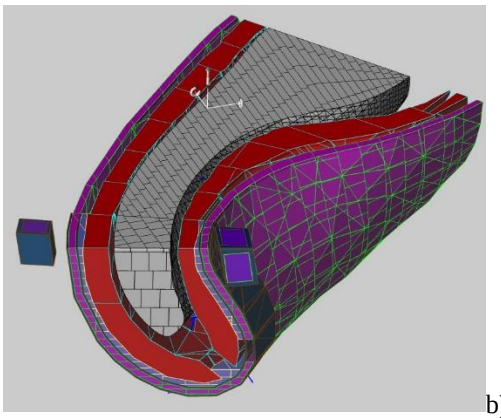

b)

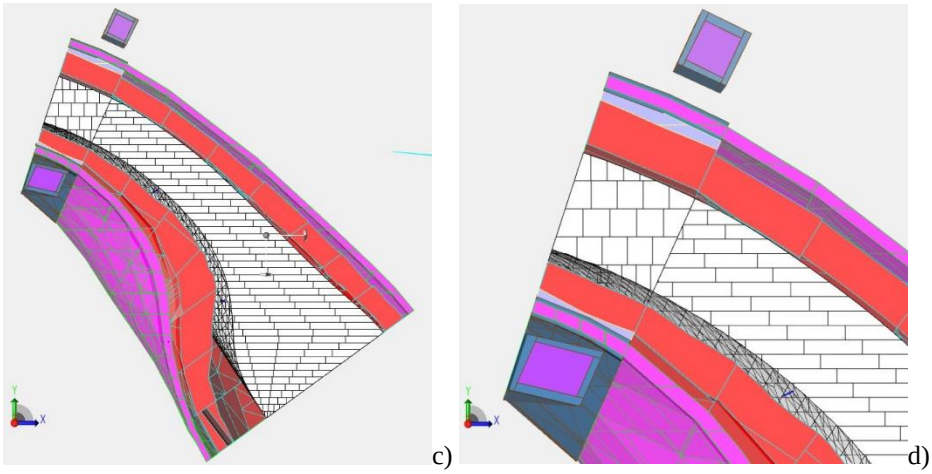

Figure 9. Neutronic model of the 36º DCLL HELIAS sector: Different views and cross sections at Z=0.

The first one represents the composition of the DCLL BB modules only, and the second one represents a mix of the BB+BSS materials, to simulate that the space is distributed to allocate the two components.

- In blue and violet two pieces of Coils, located in the Equatorial Plane at the "Inboard" and "Outboard" side of the bean-shaped Ring 8. The configuration of jacket case (blue) of Austenitic steel and a Winding pack (violet) of a mixture composition of r-epoxy 18%, Nb_3Sn 2.895%, Bronze (Cu+Sn) 7.35%, Cu 11.69%, He (liq.) 16.82%, SS316LN 43.19% and Void 0.055%, called m25, has been kept.

Voids and Lost Particles

The obtained HELIAS generic model has been then filled with void cells to complete the space devoted to the transport calculation. In MCNP code all the space must be defined to give "instructions" to the particles on the medium that they are crossing, also if such medium is filled with a void material. Thus, all the space between components has to be defined geometrically in order to don't lose particles during the transport analyses. It has been made by means of the automatic tool of SuperMC which created 2538 void cells. In Figure 10 the complex voids structures are shown

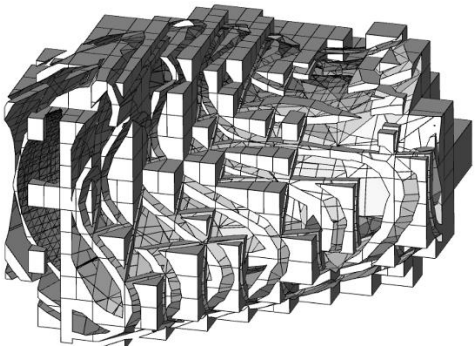

Figure 10. Voids created to fill the entire space

A final model with 5854 cells has been achieved constituted by:

- 2496 plasma cells;
- 570 cells of steel+water for VV massive layer of Rings 1-7 and the inner VV layer of Ring 8;
- 61 steel cells for the 2 VV external layers of Ring 8
- 8 steel cells for the Coil jacket;
- 139 cells for intermediate shielding layer between BB and VV at Ring 8;
- 40 cells for homogenized BB;
- 2 cells for the Coil' Winding Pack;
- 2538 void cells.

The next step has consisted in verifying the correctness of the MCNP model and fix the errors where present. This is a very consuming task since all the bugs are fixed manually. The initial number of lost particles has been 489/1e9. After some improvements and geometry fixing it has been obtained a total number of 35 lost particles over 1e9 launched being a very good results for achieving statistically reliable results. The final 35 lost particles (over 1e9 launched) are shown in Figure 9a, represented as blue rays.

The lost particles are predominantly due to a bad overlapping of surfaces. During the "MCNP input writing" task, made through SuperMC which converts the stp model to a combination of surfaces and cells of an MCNP input, in some cases the tool is not able to use the same approximation for two surfaces which are shared between 2 components creating 2 different surfaces which differ only for the last digits of the coefficients which define the surface.

3.2. Partially detailed BB DCLL HELIAS model. Adaptation from DEMO

A specific model has been developed for the assessment of the local tritium production in the breeding zone of 4 detailed BB modules and their Back Supporting Structure.

Four BB modules have been extracted from the DEMO DCLL design [13][14] and translated to HELIAS in a region

easily adaptable (a squared-shaped zone) of the Ring 8 (Figure 11a). The inclination has been modified (Figure 11b) to easily arrange the BB modules into the available space firstly by using the rotation tools of SuperMC (approximate fit) and then adjusting and modifying manually the coefficient x, y, z of the surfaces for all the components inside the MCNP input (exact fit).

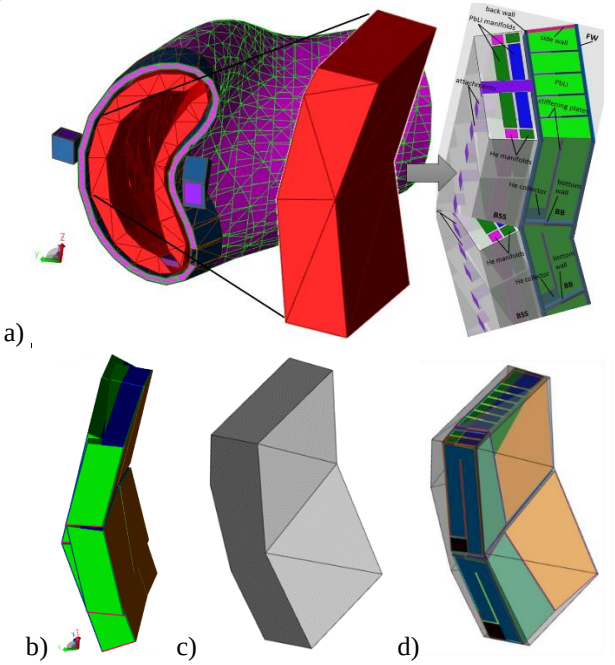

Figure 11. a) Strategy toward a semi-detailed DCLL BB design with adaptation from DEMO to HELIAS; b) rotation of 4 BB DCLL modules to insert inside a squared and massive piece (c) of the Ring 8. The realistic BB DCLL modules, keeping all the internal details (d), are introduced there. The space leftover is used as BSS.

All the details have been maintained following the realistic structure of the DEMO DCLL OB modules: First Wall, 7 PbLi channels for the inlet, 7 for the outlet, the stiffening grid, alumina FCI, Helium manifolds, side walls (left and right) and back walls. The materials used for each component as taken from the DCLL DEMO module are given in [35]. All the details of the partial model of the 4 BB modules can be also found there. The zone behind the BB modules (grey in Figure 11d) has been filled with an equivalent composition representative of the BSS (Eurofer structure + PbLi + helium, m71).

The rest of Ring 8 as the other rings are filled with the compositions simulating the total of BB+BSS (m41) and another taking into account only the BB components inside that zone (m24). The final "partially-detailed" neutronic DCLL HELIAS design is shown in Figure 12.

A comparison of the TBR results with a fully-homogenized BB zone model (model 1) has been performed to extrapolate results for a fully detailed BB model.

Such model has been also used for the assessment of the dpa in the Eurofer FW, since in the homogenized BB model the dpa could be underestimated.

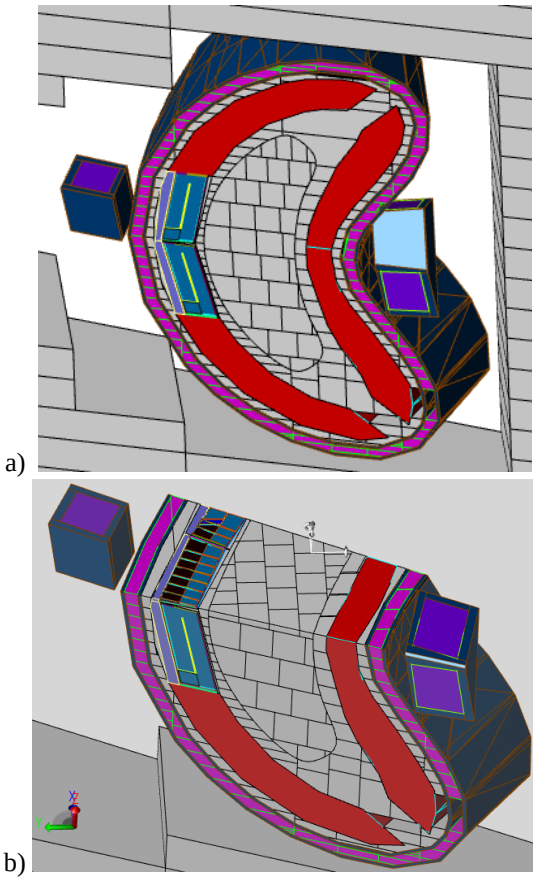

Figure 12. Ring 8 in which 4 fully detailed BB modules have been included together with a homogenized BSS. The rest (red) is homogenized composition to represent the BB or the BB+BSS.

3.3 Simplified model for NWL calculation

The NWL is the energy deposited in the first wall from the neutrons coming from plasma when crossing the first surface they encounter and without taking into account any backscattering. Thus no backscattered particles have to be computed and only incident particles are accounted. To this end, a part from the plasma, the FW and the space in between them, the rest of the model has to be voided and the importances set to 0, since no reactions have to occur there.

As the CAD model provided (Figure 3) does not included a specific model for the FW, but only a generic space left for the whole Blanket (the FW is included virtually in the neutronic model using an homogenized mixing composition) there is not a thin layer to construct the FW surface model on which it could be possible to compute and display the NWL results. So the plasma and BB models have to be used to construct such limiting FW surface. Furthermore, since in the previous models the voids were randomly created by

SuperMC with no matter if they were communicating internal and external zones of the plasma chamber, it has been re-creating voids to obtain separated void cells, those that are between the plasma and the BB, to which assign importance 1, and which constitute such boundary FW surface, and those behind the BB to which assign importance 0. No connections between the void cells inside and outside BB space are allowed. The BB importance is also set to 0, so the last values obtained are those in the last (FW) surface before the BB. Partial visualization of such model is depicted in Figure 13.

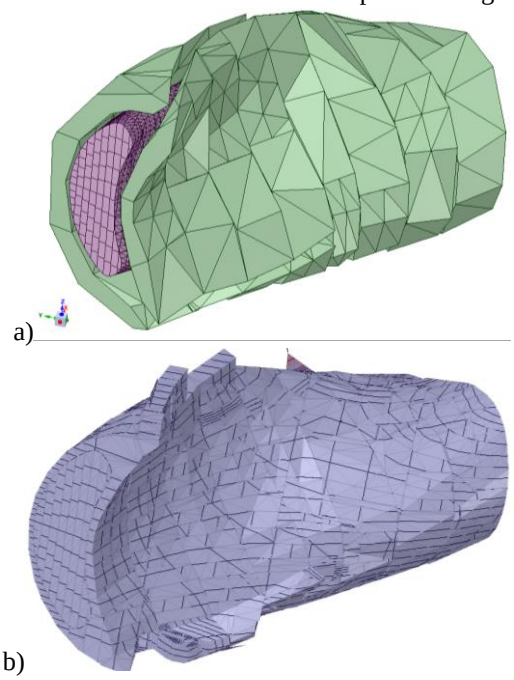

Figure 13. a) Plasma and BB zone in the simplified neutronic model devoted to NWL calculation. The region in between is filled by voids with IMP=1. b) Last surface of the model in which the NWL has to be assessed.

4. Nuclear Assessments

Particle transport calculations have been performed with MCNP5v1.6 Monte Carlo code [17] using JEFF 3.2 nuclear data library [42]. Direct simulation results have been normalized to 1.065×10^{20} n/s corresponding to the 36º sector.

Different neutronic assessments have been performed providing:

- NWL in form of different iso-value contour surfaces and 3D maps
- Plasma emission volumetric 3D maps
- Tritium production for homogenized and partially-detailed models
- Power density 3D distributions focusing on the BB regions;
- Damage/shielding responses, as 3D maps for nuclear heating, dpa and fluences focusing on VV and Coil;
- Cell results (local values) for all the responses in the relevant components: Helium and Dpa in VV, nuclear heating, dpa and neutron fluence in Coil.
- Dpa values in the FW cells for the detailed model of the 4 BB modules
- Dpa as cell values in the Winding Pack of the Coil for the detailed model in which not additional shielding is provided by using the intermediate layer.

Most of the neutronic requirements [43] adopted in DEMO seem to be reasonably applicable to stellarator devices. A recent update of the DEMO TBR target from 1.1 to 1.15 [44] could compromise the viability of an established design. Thus, it should be studied if applicable to the HELIAS case. It is urgent to define specific requirements for HELIAS, according to its maintainability, inspectability, operation scenario and remote handling requirements, among others.

4.1 Neutron Wall Loading and Plasma emission

The Neutron Wall Loading and the plasma emission as MW/m^2 have been computed for the 3D whole geometry. The representation of such responses is quite complex and different possibilities have been explored to show results that can be rightly interpreted and at the same time simple enough to be "read". Due to the 3D variations and the current technical difficulties (the lack of a single piece surface for the First Wall covering the plasma) these are given in a different format respect to the 2D profiles usually required in DEMO tokamak devices and also used in [10].

In Figure 14 the BB and plasma geometries are overlapped to the results, to make clear up to which surface the results are produced.

In Figure 15 the 3D volumetric results from the plasma to the last available surface are represented cutting at the horizontal plane z=0 and showing two perspectives, one near to Ring 8 and the other nearer to Ring 1. The scale has been enlarged up to 7 MW/m^2 to show also the emission inside the plasma. Rings 1, 2 and 3 seem to have the lower results at least in such horizontal plane. The points, farer from the plasma and in contact with the BB surface which constitute the last surface of values, correspond to the 3D NWL results.

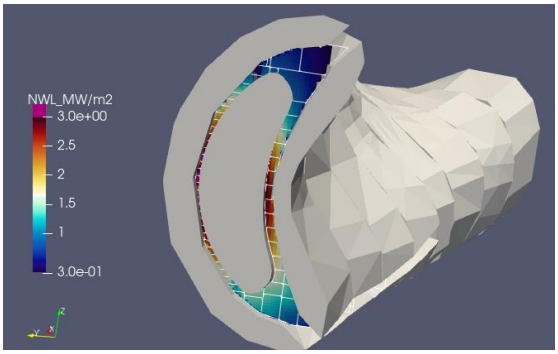

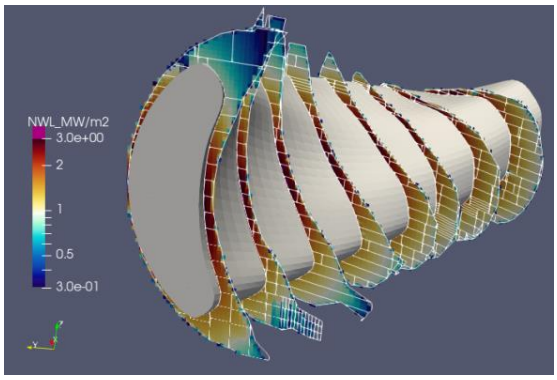

Figure 14. 3D results overlapped to the model

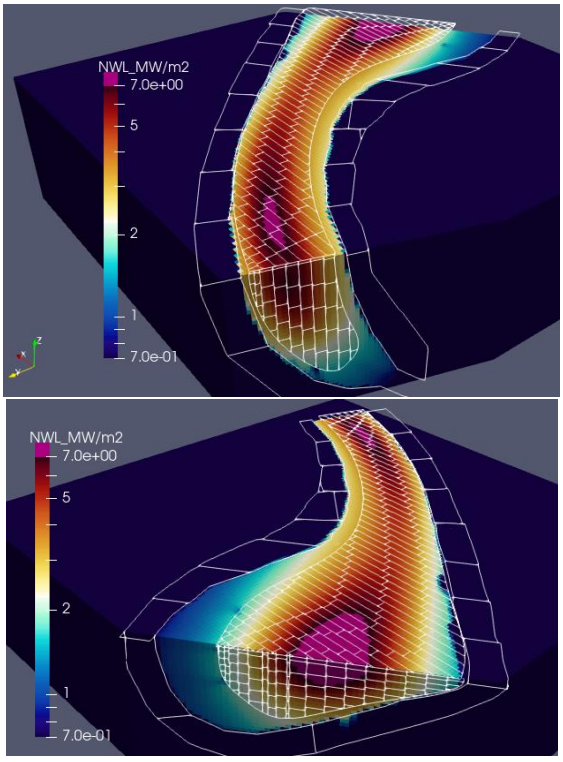

Figure 15. 3D volumetric results at z=0 showing two perspectives, one near Ring 8 and the other nearer to Ring 1.

Since it is very difficult to distinguish values for "global" zones, different contour iso-surfaces have been selected and they have been represented (Figure 16) overlapped to the geometry of the last surface to visualize only the values on the top of such surface. In black it is represented the contour 1.8 MW/m^2, then 1.6 (brown red), 1.4 (mustard), 1 (water green), 0.6 (blue) and 0.3 (deep-blue) MW/m^2. This means that a NWL slightly higher than the range 0.3-1.8 MW/m^2 can be assumed for the FW of the HELIAS design, which is in agreement with the values found in [10].

Just for a rough comparison and taking into account the due differences explained above between the two devices, the cited DCLL v3.1 developed for the DEMO2015 baseline [13][14] has a NWL in the range 0.65-1.316 MW/m^2 with an average value of 1.03 MW/m^2 [22].

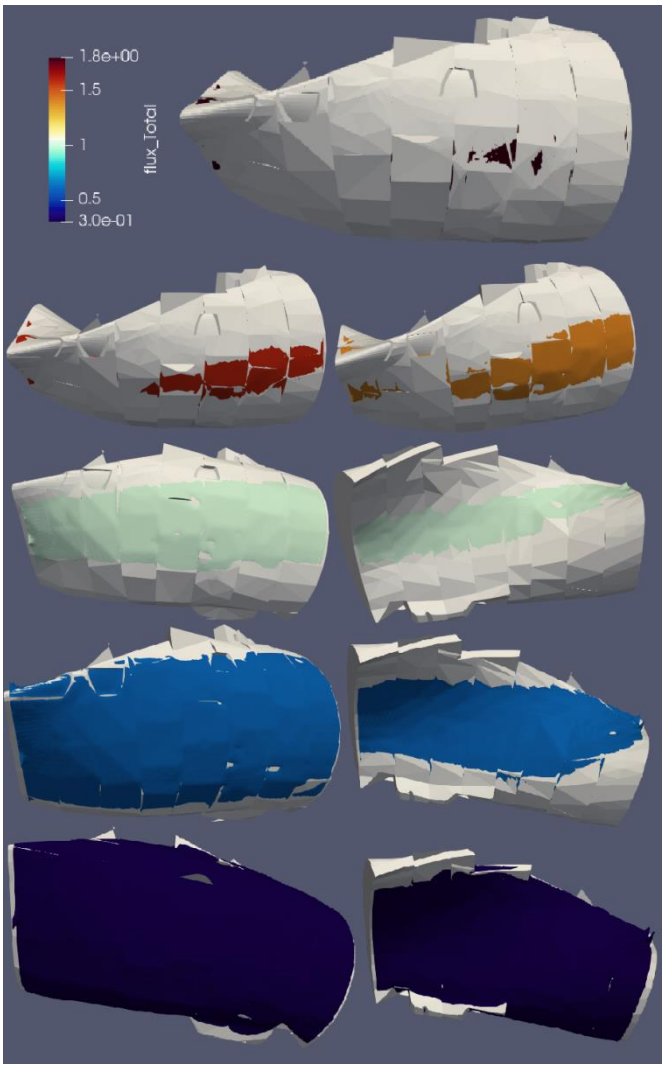

Figure 16. Contour iso-surfaces overlapped to the geometry of the last surface: 1.8 MW/m^2 (black), 1.6 (brown red), 1.4 (mustard), 1 (water green), 0.6 (blue) and 0.3 (deep-blue) MW/m^2.

4.2 Tritium Production

The priority condition for the viability of a fusion reactor which is the fuel self-sufficiency measured through the Tritium Breeding Ratio (TBR) has been evaluated. A TBR > 1 is needed for a self-sustained fusion reactor, although the allowed range to account for possible losses and uncertainties is still to be determined. The applicable requirement for DEMO taking into account a 10% of margin due to penetrations, burn-up, and uncertainties in design and cross-section data is a TBR > 1.1 [43]. Here the same target is assumed for HELIAS DCLL BB until getting a more realistic forecast about number and size of ports and penetrations which mostly affect the TBR target.

As first approach two homogenized compositions have been used to be assigned to the BB zone:

• One representative of the BB+BSS occupying all the space available for Blanket/Shield (composition m41), and
• The other representative only of the BB, i.e., all the BB space filled with a composition representing only the blankets components (composition m24).

These are considered only as preliminary approximations. In fact, as an ad hoc design for the BB and BSS has been not developed thinking on the specific requirements and characteristics of HELIAS, a different distribution between BB and BSS could be required to better fit the neutronic objectives to be achieved, among others.

The 15 cm of space between the BB zone (of 75/50 cm at OB/IB) and the VV (up to fill the total 90/65 cm of space) for Ring 8 is also used as BSS/manifold, giving to the intermediate Layer of Ring 8 a composition called m71.

The resultant TBR values for the 2 compositions m24 and m41 were 1.24 and 1.077 (Table 1), respectively, showing also local values for each ring. If we sum the contribution of the BSS intermediate layer of Ring 8 and we extrapolate the local result of BSS_R8 to Rings 1-7 (as we could employ this m71 BSS composition also for the rest of the rings) final TBR values of 1.27 and 1.11 could be obtained, respectively, considering compositions m24 and m41 for the BB+BSS modelled regions. In both cases, the target of 1.1 would be overpassed.

These results are of special interest, as it will be explained later, in view of the poor shielding performance of the current design. In fact, as the homogenization has a negative effect on the TBR result, we could expect even higher TBR when a detailed BB and BSS will be developed and implemented in the design, being the provided results conservative under this point of view.

If we select the m41 composition which represent a BB+BSS inside the Blanket region, we could still improve the shielding using a different material for the intermediate layer (m71, currently) or a part of it, still providing enough Tritium generation.

In order to have a feedback regarding the possibility of using the intermediate layer only as shielding and have the PbLi manifold only inside the BB original region, the assessments have been repeated with the model described in section 3.2 in which there are 4 detailed BB modules in Ring 8 and the rest is homogenized.

The local TBR inside the 4 BB modules plus their BSS is 4.47E-2, implying an increase of a 6% respect to the same zone homogenized (4.223E-02) using m41 composition representative of the BB and BSS components mixed together. If we extrapolate such local increase to the whole BB envelope we will increase the original TBR from 1.077 to 1.14. If the same increase due to the heterogenization is applied to the homogenized model with m24 composition it results clear that very high TBR values could be achieved (from 1.24 to 1.31).

These values (1.14 and 1.31), higher than the 1.1 target (although lower, in the first case, than the new possible target of 1.15) are encouraging regarding the possibility to avoid the use of the intermediate layer as PbLi manifold and confirm the previous prevision that it is no required for T breeding purposes. On the other side, as we will see later in the shielding assessments, this layer will result essential for shielding purposes, since a void intermediate layer would compromise very much the shielding functions. The conclusion would be to use such space as real shielding adopting better shielding materials than the adopted one for the BSS (PbLi+Eurofer).

Just to have a term of comparison the TBR for the heterogenized DCLL v3.1 of DEMO 2015 was 1.196. Furthermore, a similar difference in the TBR result (of a 6.7%) was found [26] between the homogenized and heterogenized models of the DCLL v3.1 for DEMO.

Table 1. TBR results for homogenized BB+BSS (m41) and only homogenized BB (m24) occupying the whole BB region, and extrapolating the use of a BSS/manifold intermediate layer (m71) from the Ring 8 to the rest of rings

Ring	m24 (BB)	m71 (BSS) interm. layer	m41 (BB+BSS)	m71 (BSS) interm. layer
1	1,15E-01	*2,85E-03**	1,01E-01	*3,10E-03**
2	1,42E-01	*3,52E-03*	1,22E-01	*3,77E-03*
3	1,45E-01	*3,62E-03*	1,25E-01	*3,87E-03*
4	1,49E-01	*3,70E-03*	1,28E-01	*3,96E-03*
5	1,66E-01	*4,13E-03*	1,44E-01	*4,44E-03*
6	1,72E-01	*4,29E-03*	1,49E-01	*4,61E-03*
7	1,77E-01	*4,41E-03*	1,54E-01	*4,74E-03*
8	1,77E-01	4,40E-03	1,53E-01	4,73E-03
TBR BB	**1,24**		**1,077**	
TBR BB+ interm layer[1]	**1,27**	3,09E-02	**1,110**	3,32E-02

[1]TBR in intermediate layer R8 calculated; **R1-7 extrapolated*

4.3 Nuclear Heating in BB/BSS zone

3D mesh tallies distributions have been produced for the whole reactor to show in very general terms the Nuclear Heating performances of the entire machine. Specific results for the BB+BSS regions are presented in Figure 17.

The entire 36º half-sector has been covered with a resolution of 60 bins of 25cm in the X direction, 50 bins of 34 cm in the Y direction and 42 bins of 25 cm in Z direction, for a final mesh of 126.000 voxels of 25x34x25 cm^3. Two different views showing vertical and horizontal cuts are shown in Figure 17 separating the component for neutron and photons heating generation.

The results are referred to the actual composition of the structures, being mainly mixture compositions.

The figures allow showing the most irradiated zones, being mainly the equatorial "OB" zone for Rings 8-7 and equatorial "IB" for Rings 4-5. An important streaming effect is also observed in the Upper and Lower Ports regions in which no plugs are yet located.

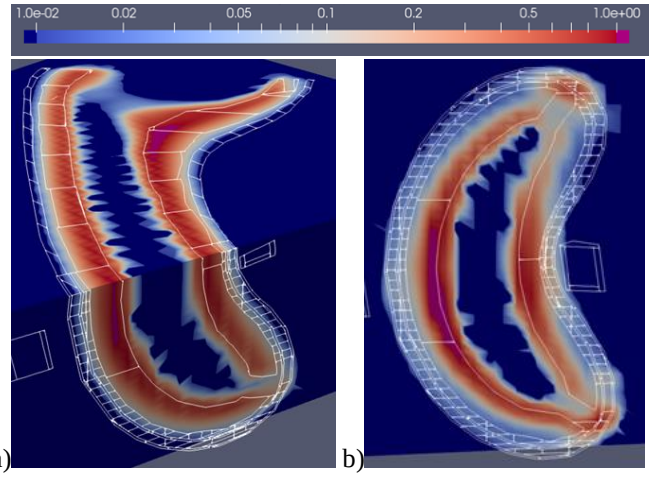

Figure 17. Mesh tally radial-poloidal-toroidal 3D distribution of the Nuclear Heating (W/cm^3) in the whole DCLL HELIAS BB+BSS structures, neutron (a) and γ (b) component.

4.4 Shielding and damage responses

The plasma confinement can be kept only without overpassing the quench limits posed on the Superconducting Coils [45]. Furthermore, damage limits are imposed to the Vacuum Vessel (VV), to maintain its integrity [46] and other recommendations are considered for its possible re-welding [47].

4.4.1 Nuclear Heating

A rough evaluation of the shielding efficiency of the DCLL preliminary design for HELIAS has been performed. For that, the nuclear heating in the reactor components needs to be assessed, paying special attention, in this case, to the power density on the coil conductor at the zone nearest to the plasma.

The NH has been calculated as tally cell results in different VV and Coils zones at both the IB and OB equatorial regions of Ring 8, as shown in Table 2 and 3 for the composition of the BB zone m24 and m41, respectively. Results are also given for cells occupying the IB and OB equatorial zone of the Massive VV of Ring 7, for both compositions of the BB zone (m24 and m41) as in Table 4.

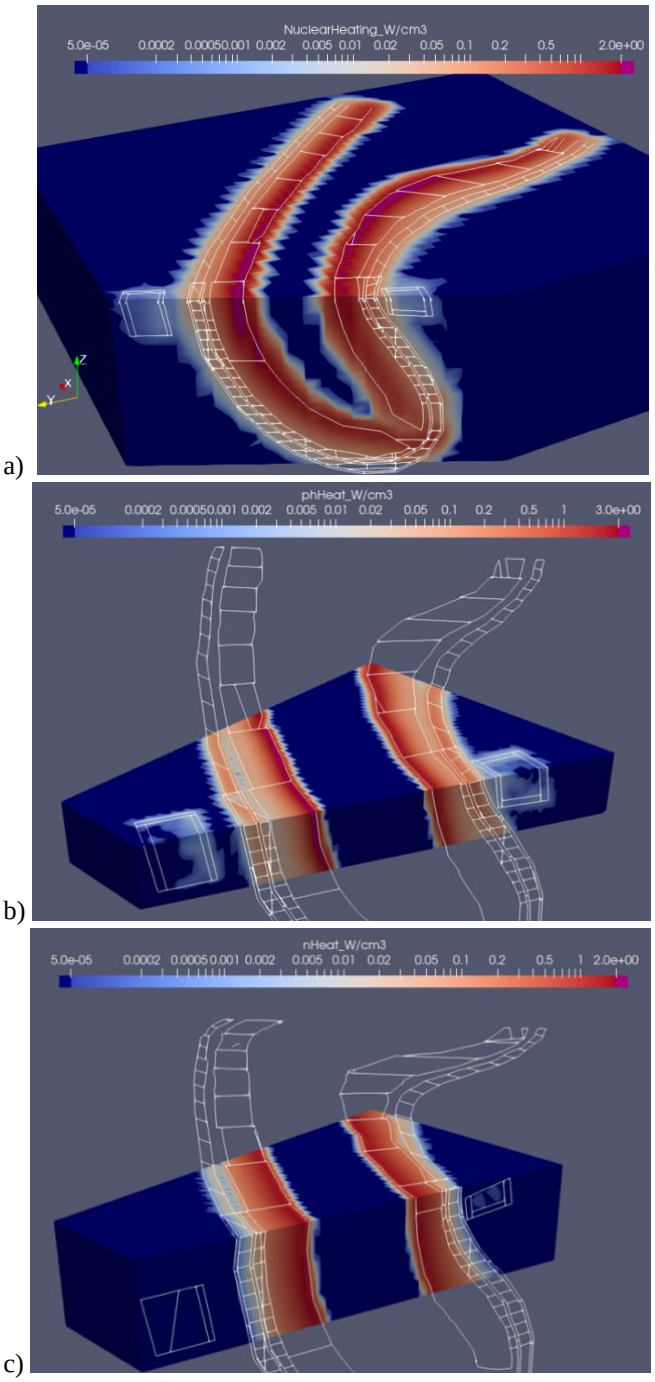

Figure 18. Mesh tally radial-poloidal-toroidal 3D distribution of the Nuclear Heating (W/cm^3) in the whole HELIAS structures: photons and neutron contributions. Different resolution for rings is used.

Furthermore, mesh tally 3D maps have been produced in all the reactor structures, giving separated 3D maps for neutron and photon contribution to the total nuclear heating (Figure 18). The model with m24 composition to fill the whole BB envelope has been used. Two different resolutions have been adopted:

- One to show more specific results for Rings 8 and 7, with voxels of 10 cm x 10 cm x 10 cm resolution in XYZ directions, and
- Another more general covering all Rings 1 -8. In this case, the entire 36º half-sector has been studied with a resolution of 60 bins of 25 cm in the X direction, 50 bins of 34 cm in the Y direction and 42 bins of 25 cm in Z direction, for a final mesh of 126.000 voxels.

The scale has been limited to $5x10^{-5}$ W/cm^3 which is the maximum value before producing the Coil quench, indicating that only values under the scale (in deep-blue colour) would satisfy the requirements.

According to both the tables and Figures, it can be seen that the values inside the winding pack (WP) are about 1 order of magnitude (~2-6 x 10^{-4} W/cm^3) higher than the limit, depending on IB/OB zones and m24/m41 models (look at Tables 2 and 3).

From Figures 17 and 18, values around 5 W/cm^3 can be expected at the FW. These could be higher if it is considered that the BB model does not include a separate FW, but is homogenized. Just for comparison, values around 7 W/cm^3 [14][22] were found at the FW of the DCLL v3.1 DEMO.

4.4.2 Neutron Fluence

Other fundamental requirements to be observed [45] are relative to the total and fast (E> 0.1 MeV) fluence in different parts of the Coil.

Neutron fluences have been calculated again as cell values (for model with m24 and m41 BB compositions) and as mesh tallies 3D maps (only for model using m24 BB composition).

Total, low and fast neutron fluences cell values are given in the Table 2 (for m24, in cells of VV and Coil of Ring 8), in Table 3 (for m41, in cells of VV and Coil of Ring 8) and in Table 4 (for both models using m24 and m41 for VV cells of Ring 7) while only integral neutron fluence is given in the 3D maps (Figure 19).

The values are provided as n/cm^2 per Full Power Year (FPY). Hence, the results have to be multiplied by 6 FPY if the same lifetime than the adopted for DEMO [48] is considered also for HELIAS. Otherwise, a different operational scenario can be suggested to accomplish the quench limits (and also the structural/damage limits that we will see later).

If the 6 FPY schedule is assumed, it can be observed that the values inside the winding pack are fully accomplished adopting m41 composition or very near to be fulfilled when adopting m24 composition.

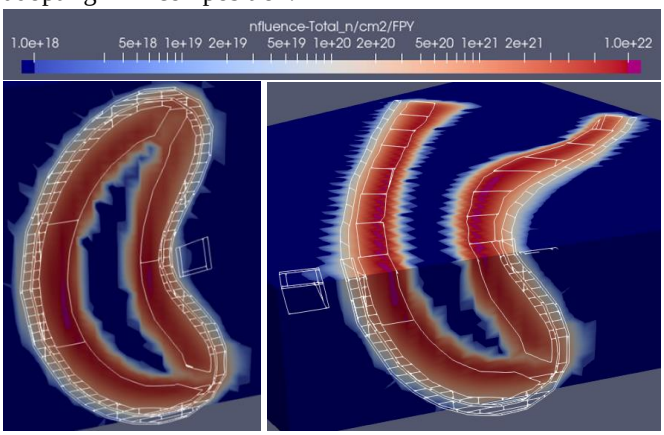

Figure 19. Mesh tally radial-poloidal-toroidal 3D distribution of the neutron fluence (n/cm^2/FPY) in the whole HELIAS structures. Values below the scale (deep blue) would comply with the quench limit ($1x10^{18}$ n/cm^2)

From Figure 19 values of about $2x10^{22}$ n/cm^2/FPY are expected to the FW, being very similar to those observed in DEMO DCLL v3.1 [14][22].

Table 2. Shielding responses in Ring 8 of HELIAS DCLL design using BB composition m24 (homogenization of the BB components only). The BSS is included in the intermediate shielding layer as m71 composition.

	LIMITS:	2.75 dpa VV/ 10^{-4} dpa WP		1appm VV		5^{-5} W/cm^3	10^{18} n/cm^2			
							Neutron fluence (n/cm^2/y)			
Model BB m24		DPA/y m50/m25	DPA (x6FPY)	appm He/y m50/m25	appm He (x6FPY)	Nuclear Heating W/cm^3	E< 0.1MeV	E> 0.1MeV	total	n/cm^2 (x6FPY)
VV OB	VV1 (Steel)	5,20E-02	3,12E-01	2,58E-01	1,55E+00	1,13E-01	3,24E+20	1,76E+20	5,00E+20	
	VV inside (Water+Steel)	5,18E-03		5,63E-01		8,16E-02	7,69E+19	1,61E+19	9,31E+19	
	VV2 (Steel)	2,75E-03	1,65E-02	3,30E-02	1,98E-01	1,87E-02	1,73E+19	9,13E+18	2,65E+19	
Coil OB	Jacket front	7,71E-04		2,93E-03		2,85E-03	3,52E+18	2,84E+18	6,37E+18	
	Jacket L	2,78E-05		1,17E-04		2,85E-04	8,51E+16	9,99E+16	1,85E+17	
	Jacket L	3,74E-04		1,92E-03		2,21E-03	1,50E+18	1,35E+18	2,85E+18	
	WP	8,53E-05	5,12E-04	5,33E-04		3,79E-04	6,66E+17	2,57E+17	9,23E+17	1,54E+18
	Jacket rear	7,00E-06		3,96E-05		7,85E-05	4,81E+16	3,44E+16	8,25E+16	

VV IB	VV1 (Steel)	1,91E-01	1,14E+00	9,42E-01	5,65E+00	3,92E-01	9,76E+20	6,44E+20	1,62E+21
	VV inside (Water+Steel)	2,64E-02		2,31E+00		3,35E-01	3,17E+20	7,98E+19	3,96E+20
	VV2 (Steel)	7,91E-04	4,75E-03	2,37E-02	1,42E-01	3,17E-02	5,05E+18	2,24E+18	7,30E+18
Coil IB	Jacket front	3,94E-04		1,99E-03		4,85E-03	1,69E+18	1,30E+18	3,00E+18
	Jacket L	1,11E-04		8,40E-04		1,57E-03	4,71E+17	3,35E+17	8,06E+17
	Jacket L	1,76E-04		2,25E-03		3,17E-03	8,29E+17	4,95E+17	1,32E+18
	WP	6,72E-05	4,03E-04	4,75E-04		6,01E-04	4,47E+17	1,80E+17	6,27E+17	1,08E+18
	Jacket rear	8,84E-05		9,40E-04		1,15E-03	3,61E+17	2,44E+17	6,05E+17	

Table 3. Shielding responses in Ring 8 of HELIAS DCLL design using BB composition m41 (BB+BSS components homogenized together). Material m71 is also used for the intermediate shielding layer.

	LIMITS:	2.75 dpa VV/ 10^{-4} dpa WP		1appm VV		5^{-5} W/cm^3	10^{18} n/cm^2			
						Nuclear	Neutron fluence (n/cm^2/y)			
Model BB+BSS m41		DPA/y m50/m25	DPA (x6FPY)	appm He/y m50/m25	appm He (x6FPY)	Heating W/cm^3	E < 0.1MeV	E > 0.1MeV	total	n/cm^2 (x6FPY)
VV OB	VV1 (Steel)	3,82E-02	2,29E-01	2,42E-01	1,45E+00	1,05E-01	3,26E+20	1,31E+20	4,58E+20	
	VV inside (Water+Steel)	3,60E-03		4,93E-01		7,07E-02	6,72E+19	1,12E+19	7,84E+19	
	VV2 (Steel)	1,91E-03	1,15E-02	3,01E-02	1,81E-01	1,66E-02	1,63E+19	6,78E+18	2,31E+19	
Coil OB	Jacket front	5,07E-04		2,10E-03		2,56E-03	3,02E+18	1,94E+18	4,96E+18	
	Jacket L	1,73E-05		8,84E-05		1,83E-04	8,38E+16	6,98E+16	1,54E+17	
	Jacket L	2,66E-04		1,44E-03		2,08E-03	1,39E+18	9,88E+17	2,38E+18	
	WP	5,33E-05	3,20E-04	4,13E-04		2,89E-04	5,10E+17	1,58E+17	6,68E+17	9,50E+17
	Jacket rear	2,70E-06		5,83E-05		6,74E-05	4,52E+16	1,23E+16	5,74E+16	
VV IB	VV1 (Steel)	1,68E-01	1,01E+00	8,10E-01	4,86E+00	3,71E-01	1,14E+21	5,96E+20	1,74E+21	
	VV inside (Water+Steel)	2,03E-02		2,14E+00		3,07E-01	2,91E+20	6,17E+19	3,53E+20	
	VV2 (Steel)	5,53E-04	3,32E-03	1,80E-02	1,08E-01	2,71E-02	3,87E+18	1,53E+18	5,40E+18	
Coil IB	Jacket front	2,49E-04		1,71E-03		4,04E-03	1,23E+18	8,03E+17	2,04E+18	
	Jacket L	6,85E-05		4,40E-04		1,23E-03	3,10E+17	2,42E+17	5,52E+17	
	Jacket L	1,12E-04		1,56E-03		2,85E-03	5,98E+17	3,21E+17	9,18E+17	
	WP	4,34E-05	2,60E-04	3,81E-04		4,18E-04	2,87E+17	1,12E+17	4,00E+17	6,73E+17
	Jacket rear	6,59E-05		5,84E-04		1,06E-03	2,28E+17	1,92E+17	4,20E+17	

Table 4. Shielding responses in Ring 7 of HELIAS DCLL design using BB composition m24 and m41. The intermediate layer in this case is void. Having no Coil around this ring, only the VV (1 massive water+steel layer) has been studied. The cells correspond to the eq. zone at IB and OB positions.

Cells Values at the eq. zones		Model BB (m24)				Model BB+BSS (m41)			
		dpa m50	x6FPY	appm He m50	X 6FPY	dpa m50	x6FPY	appm He m50	X 6FPY
Ring 7	OB Massive VV	1,80E-02	1,08E-01	1,24E+00	7,45E+00	1,24E-02	7,47E-02	1,15E+00	6,91E+00
	IB Massive VV	5,15E-02	3,09E-01	2,88E+00	1,73E+01	3,72E-02	2,23E-01	2,70E+00	1,62E+01
	LIMITS:		2.75 dpa		1appm He		2.75 dpa		1appm He

4.4.3 Helium production and radiation damage

The last requirements referred as structural requirements and also one of the requirements to avoid the coil 'quench' are relative to helium production (appm He) [47] and radiation damage (dpa) [45][46].

The helium production has been calculated as tally cell results at both the IB and OB equatorial regions of the 3 layered VV of the Ring 8, as shown in Table 2 and 3 for the composition of the BB zone m24 and m41, respectively, and of the massive VV of the Ring 7 as shown in Table 4.

Only few zones of the VV fulfil the recommended limit of 1 appm [47] accumulated during 6 FPY. This is considered as limit for re-welding, but this is only a recommendation since no re-welding is foreseen for the VV at this moment. The

lower values again are encountered in the OB side, in the 2nd VV layer and in the configuration m41.

The dpa has been assessed as cell results in IB and OB mid-plane cells of the VV and coil because these are the most critical zone. As the dpa is critical not only for the Coil and VV [45] [46] but also for the Eurofer FW [43][46], 3D maps have been produced for both the EUROFER (Figure 20a), selecting a scale adequate to represent results of the zones in which will be located Eurofer components, that is from the FW to the BSS, and for the austenitic steel SS316LN (Figure 20b) modifying the scale to shows the values from the VV to the Coil.

In Figure 20a it is possible to observe that the Eurofer located in the FW would be subjected to a damage around 9 dpa/FPY, being lower than the two targets of 20 and 50 dpa (for the two BB operations phases [48]) when we accumulate the value during the 1.57 FPY or 4.43 FPY operation times foreseen for DEMO and applied also to HELIAS for having a realistic framework for comparison.

The lack of a detailed representation of the FW, with a W coating covering the He-cooled Eurofer FW layer, could produce dpa results different from the actual ones. In order to avoid such a misleading interpretation, the detailed BB model of the 4 blankets modules, as developed in the semi-detailed model, has been used to calculate the dpa in the FW Eurofer structure of the 4 modules, giving the values summarized in Table 5.

Values between 13 and 15 dpa/FPY are obtained, implying a slight increase of the values obtained with the homogenized blanket modules. This would compromise a bit the foresee operation since the 1.57 FPY at 20 dpa would be overpassed.

For comparison, the maximum value achieved at the FW of DCLL v3.1 DEMO was 12.23 dpa/FPY [14][22].

Regarding the dpa in VV and Coil, according to the 3D maps produced, as well as according to the dpa cells values recollected in Table 2 and 3, the limit of 2.75 dpa for VV is fulfilled in all the configurations.

The limit of $\leq$0.5-1x10^{-4} dpa for Coil quench is not fulfilled since the accumulated dpa during the 6 FPY reactor operation is around 2-5 x10^{-4} dpa. Such prevision is similar if we observe the 3D results in the Coil WP shown in Figure 20b.

If we look at the values calculated using detailed model of 4 BB and without Shielding intermediate layer in Ring 8 in which the Coil is located, we found inclusive higher values of around 8-9 x10^{-4} dpa (obtained by multiplying by 6 FPY the values of Table 5).

The values at the VV of Ring 7 in which intermediate layer is suppressed (voided in the generic homogenized model) are also given in Table 4. Although the dpa results are well below the limit, the high He production confirm the usefulness of an ad-hoc shielding material to fill this region.

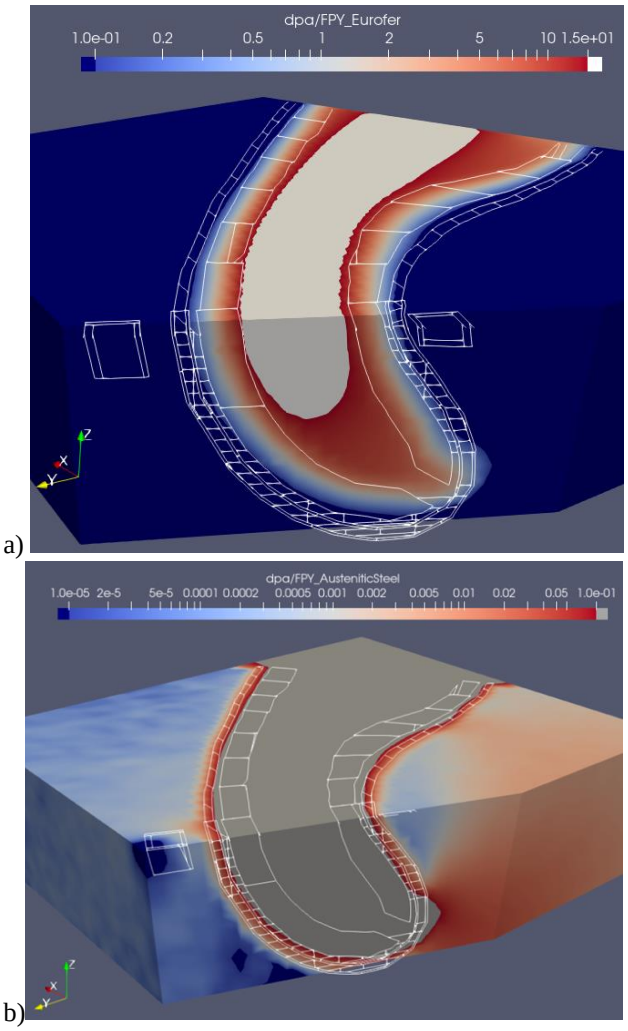

Figure 20. Mesh tally radial-poloidal-toroidal 3D distribution of the displacement per atom (dpa/FPY) in the whole DCLL HELIAS structures, a) for Eurofer and b) for Austenitic steel. In figure b) values higher than the scale (>2.8 dpa in grey) indicates steel areas deeply damaged, and values below the scale (<10^{-4} dpa in deep blue) indicate if the WP Coil would comply with the quench limit when integrated during 6FPY.

Table 5. Dpa/FPY values in FW and WP using detailed model of 4 BB and without shielding intermediate layer in Ring 8 in which the Coil is located

FW	m5		dpa/FPY
		Module 1 up	13,91
		Module 1 down	15,26
		Module 2 down	15,14
		Module 2 up	14,43
WP	m25		dpa/FPY
		OB	1,60E-04
		IB	1,32E-04

5. Discussion and Conclusions

Substantial progress has been made in understanding stellarator plasmas and important advancements have been already obtained on the physics aspects. To follow on the conceptualization of a mature HELIAS reactor, different engineering and technological aspects have to be studied, improved and solved. Guiding onto the conceptual design process, a neutronic design of the reactor has been developed starting from a test design called "HELIAS 5-B" with a fusion power of 3000 MW.

Simplified neutronic models with DCLL Breeding Blanket, taken in its essence from the DEMO project, have been developed to perform preliminary neutronic assessments in order to demonstrate the viability of this breeding concept for a stellarator, and to pushing in the conceptual design of such a complex machine.

The challenges of the neutronic 3D modelling and 3D analyses peculiarity of the stellarator devices have been addressed.

The development of an apparently simple neutronic design starting from the CAD model of an HELIAS stellarator, in which most of the components are homogenized, is a very hard and time-consuming process. This is due to the inherent complexity of the stellarator original CAD design which is fully made by splines. This bottleneck will also be addressed in future developments by studying better CAD modelling solutions.

Using the SuperMC code tools, the simplification of the CAD model has been pursued and it has been adapted to the MCNP code in terms of splines approximation to faceted surfaces, void creation and decomposition, gluing of pieces of the same component, and splitting of others

Different models have been created, each one specifically focused on the analyses to be performed with it.

A generic model including a homogenized BB envelope, a 3 layers VV in one of the rings and a simplified model of Coil in the IB and OB equatorial zone has been created for shielding assessments purposes. This has been also used for TBR assessment to compare with a partial detailed model of DCLL BB: in such semi-detailed model 4 BB modules are completely heterogenized and the rest is represented with a homogenized composition. Two different homogenized compositions have been employed for the generic space surrounding the plasma that would represent the BB structures: one representing only the DCLL BB modules, and another representing both the BB and the BSS/manifold structures. In both models, the space left between the BB zone and the VV has been filled with materials representative of the BSS/manifolds/Shields, since such initially void space was unnecessary and could be better exploited.

Lastly, a specific model has been used for the calculation of the NWL, modifying the provided CAD to construct a limiting FW surface to which assign importance 1 for obtaining the results.

Due to the 3D variations and the lack of a single piece surface for the First Wall covering the plasma, many different plots have been produced to give a comprehensive representation of the 3D NWL variation. A NWL slightly higher than the range 0.3-1.8 MW/m^2 is obtained for this HELIAS configuration. The direct emission from plasma has been also depicted to show the differences between rings, among others.

As preliminary conclusion derived from these first assessments, it results that the most exposed region (and thus, the zones in which the shielding and damage protection could be a main issue) are the equatorial "OB" zones for Rings 8-7 and equatorial "IB" zones for Rings 4-5. Due to this fact, the simpler 2D radial profiles calculated in the IB equatorial plane for tokamak conservative studies, are not applicable in the complex stellarator configuration. Complete 3D distributions for all the responses have been produced to answer the complex specific challenges of a stellarator. In fact, due to the more complicated nature of stellarator, it resulted indispensable to perform 3D neutronics analyses to adequately represent the variation of the neutronic responses also in the toroidal direction. This is considered essential to understand the general behaviour of the different zones under irradiation, since it resulted no so obvious, like in tokamak, which are the most affected zones.

The analyses have involved the shielding responses on the Vacuum Vessel and on the Coil located around the bean-shaped Ring number 8, namely, neutron fluence, nuclear heating, dpa and helium production. Local accumulated results inside cells as well as 3D distribution maps have been produced to represent adequately the 3D variation of the stellarator configuration. The nuclear heating values inside the winding pack are about 1 order of magnitude (~2-6 x 10^{-4} W/cm^3) higher than the limit, depending on IB/OB zones and the kind of BB representation: BB vs. BB+BSS inside the BB space. Regarding the neutron fluence, if the 6 FPY schedule is assumed, it can be observed that the values inside the winding pack are fully accomplished adopting BB+BSS composition or very near to be fulfilled when adopting only BB composition inside the blanket region. Nevertheless, the dpa at such locations is 3-5 times higher than the quench limit.

Responses such as the nuclear heating and the dpa have been also calculated for the whole BB region. More precise dpa results have been provided for the FW of 4 detailed BB modules taken from the partial detailed model. Values between 13 and 15 dpa/FPY are obtained implying a slight increase of the values obtained with the homogenized blanket modules. This would compromise a bit the foresee operation since the 1.57 FPY at 20 dpa would be overpassed.

TBR values around 1.27 and 1.1 have been obtained in the two homogenized configurations, BB vs. BB+BSS,

respectively, fulfilling in both cases the 1.1 TBR target, and values of 1.24 and 1.077 would be the correspondent ones in case in which the intermediate layer would be left to shielding purposes instead than to PbLi collecting (breeding also Tritium). Higher values (+6%) around 1.31-1.14 could be expected, as they have been extrapolated, by using the detailed description of the DCLL BB modules and BSS instead of the homogenized one.

Such encouraging values will allow making important improvements on the lacking shielding performance of such preliminary DCLL HELIAS design. The use of the intermediate shielding layer resulted in fact essential to achieve better shielding performances, while not necessary to be employed as manifold for PbLi since a satisfying TBR would be obtained. Improvements on such intermediate layer are considered essential to protect both the VV and the Coil, that at the moment are subjected to high neutron radiation in some points, causing slightly high nuclear heating and damage.

A recent study carried out using a HCPB BB [11] [49] reaches very similar conclusions about the lack of adequate shielding, implying that one of the main reason is the limited space available and should be overcome by improved design solutions for blanket and shield.

It has to be emphasized that the current analyses are on very raw design developed with the aim of having a preliminary idea of the nuclear performances and viability of the DCLL concept for a stellarator device. In the next future, the crucial step will be to develop a dedicated DCLL BB design that takes the essence of the DCLL DEMO and adapts and improves it considering the peculiarities and needs of HELIAS.

Furthermore, as an ad hoc design for the BB and BSS has been not developed thinking on the specific requirements and characteristics of HELIAS, a different segmentation from the MMS/SMS one and a new distribution between BB and BSS could be required to better fit the neutronic objectives to be achieved. Novel activities addressing these issues will be developed among the Prospective R&D (PRD) FP9 EUROfusion Programme for the period 2021-2025.

Acknowledgements

This work has been carried out within the framework of the EUROfusion Consortium and has received funding from the Euratom research and training programme 2014-2018 and 2019-2020 under grant agreement No 633053. The views and opinions expressed herein do not necessarily reflect those of the European Commission. The authors acknowledge the funding by Community of Madrid (TechnoFusión (III)-CM (S2018/EMT-4437) project co-financing with Structural Funds (ERDF and ESF)).

The authors would like to thank the FDS Team for providing an improved SuperMC version.

References

[1] F. Warmer, et. al, Fusion Eng. Des.123 (2017) 47–53
[2] T. Donné, European Research Roadmap to the Realisation of Fusion Energy, ISBN 978-3-00-061152-0, www.euro-fusion.org/eurofusion/roadmap
[3] F. Schauer, et al., HELIAS 5-B magnet system structure and maintenance concept, Fus. Eng. Des. 88 (2013), 1619-1622
[4] U. Fischer, et al., Final Report on Deliverable DS 2.2.1 2018, EFDA_D_2LGBB3, 30-01-2019
[5] El-Guebaly, L A. Neutronics analysis of the modular stellarator power reactor UMTOR-M. United States, 1983.
[6] L. A. El-Guebaly, "Neutronics analysis for the stellarator power plant study SPPS," Proceedings of 16th International Symposium on Fusion Engineering, Champaign, IL, USA, 1995, pp. 1162-1165 vol.2, doi: 10.1109/FUSION.1995.534432.
[7] S Zimin, at al., Overview of Australian activities of fusion neutronics, Fusion Eng. Des., Volume 45, 1999, 117-126
[8] L.A. El-Guebaly, et al., Nuclear challenges and progress in designing stellarator fusion power plants, Energy Conversion and Management, Volume 49, July 2008, Pages 1859-1867
[9] A. Häußler, et al., Verification of different Monte Carlo approaches for the neutronic analysis of a stellarator, Fus. Eng. Des., 124 (2017), pp. 1207-1210
[10] A. Häußler, et al., Neutronics analyses for a stellarator power reactor based on the HELIAS concept, Fus. Eng. Des, 136 (2018) 345-349
[11] A. Häußler, et al., Use of mesh based variance reduction technique for shielding calculations of the stellarator power reactor HELIAS, Fus. Eng. Des.146, (2019) 671-675
[12] Jin-YangLi, et al., Neutronics analysis of the stellarator-type fusion-fission hybrid reactor based on the CAD optimization method, Annals of Nuclear Energy, 150 (2021) 107846
[13] I. Palermo, et. al, Fusion Eng. Des. 138 (2019) 217–225
[14] I. Fernández, I. Palermo, F. R. Urgorri, DCLL Design Report 2017, EFDA_D_2ND27P, 2018
[15] Y. Wu, et al. CAD-Based Monte Carlo Program for Integrated Simulation of Nuclear System SuperMC, Annals of Nuclear Energy 82(2015) 161-168
[16] CATIA v5 ©2002-2021 Dassault Systèmes
[17] X-5 Monte Carlo Team, 'MCNP – A general Monte Carlo N-Particle Transport Code, Version 5'
[18] D. Rapisarda, et al., Overview of DCLL research activities in the EU/Spain, Proceeding of 26th IEEE SOFE, Austin, TX, 2015, pp. 1-8, doi: 10.1109/SOFE.2015.7482358
[19] D. Rapisarda, et al., Conceptual Design of the EU-DEMO dual coolant lithium lead equatorial module, Trans. Plasma Sci. 44 (2016) 1603–1612. 111
[20] I. Palermo, et al., Neutronic analyses of the preliminary design of a DCLL blanket for the EUROfusion DEMO power plant, Fusion Eng. Des. 109–111 (2016) 13–19.
[21] I. Palermo, et al., Tritium production assessment for the DCLL EUROfusion DEMO, Nucl. Fusion 56 (2016) 104001.
[22] I. Palermo, et al., Optimization process for the design of the DCLL blanket for the European DEMOnstration fusion reactor according to its nuclear performances, Nucl. Fusion 57 (2017) 076011.
[23] D. Rapisarda, et al., Status of the engineering activities carried out on the European DCLL, Fusion Eng. Des. 124 (2017) 876–881.

[24] I. Fernandez, et al., DCLL Design Report 2015, EFDA_D_2MYHGZ v1.0/BB-4.2.1-T002-D001 (2016).
[25] I. Fernández, I. Palermo, F. R. Urgorri, L. Maqueda, D. Alonso, J. Olalde, DCLL Design Report, (2016) EFDA_D_2MMM6Q, 2017.
[26] I. Fernández, I. Palermo, F. R. Urgorri, D. Rapisarda, DCLL Design Report 2018, EFDA_D_2NTWTN, 2019
[27] Iván Fernández-Berceruelo, Iole Palermo, et al., Alternatives for upgrading the EU DCLL breeding blanket from MMS to SMS, Fus Eng Des, Proceeding SOFT 2020, (accepted)
[28] R. Wenninger, DEMO1 Reference Design—'EU DEMO1 2015, (2015) https://idm.euro-fusion.org/?uid=2LBJRY.
[29] P. Pereslavtsev, Generic DEMO Model for MCNP, (2015) https://idm.euro-fusion.org/?uid=2L6HJ7.
[30] J. Harman, DEMO Fusion Power Plant, Plant Requirements Document (PRD), EFDA_D_2MG7RD, (2014).
[31] L.V. Boccaccini et al., Objectives and status of EUROfusion DEMO blanket studies, Fusion Eng. Des., Volumes 109–111, Part B, 1 November 2016, Pages 1199-1206
[32] R. Kemp 2012 DEMO1_July_12, EFDA_D_2LBVXZ
[33] DEMO1 PROCESS output, 2017, EFDA_2NDSKT
[34] A. Häußler, HELIAS_CAD_data.stp, 5th December 2017
[35] U.Fischer, A. Häußler, G. Bongioví, I. Palermo, F. Mota S2-3.01-T002-D001: DS2.2.1.2018 BB and Neutronics (KIT, CIEMAT) EFDA_D_2LGBB3
[36] I. Palermo, et al., Divertor options impact on DEMO nuclear performances, Fusion Eng. Des. 130 (2018) 32–41
[37] SpaceClaim Engineering 2014, www.SpaceClaim.com
[38] Paraview 5.7 https://www.paraview.org/ ParaView: An End-User Tool for Large Data Visualization, Visualization Handbook, Elsevier, 2005, ISBN-13: 978-0123875822
[39] A Häußler, U. Fischer and F. Warmer, Neutronics source modeling for stellarator power reactors of the HELIAS-type, Compact at the 47th Annual Meeting on Nuclear Technology (AMNT) 2016, Hamburg, Germany, helias_source.f90
[40] F. Warmer, HELIAS_COIL_HM1.stp, 2019
[41] I. Palermo, S2-WP19.2-T002-D001: Stellarator breeding blanket studies (2019) (CIEMAT) EFDA_D_2MVLTZ
[42] The JEFF-3.2 Nuclear Data Library, NUCLEAR ENERGY AGENCY, OECD, 2014
[43] U. Fischer, et al., Fusion Eng. Des. 98–99, 2015
[44] U. Fischer et al., Required, achievable and target TBR for the European DEMO, Fusion Eng. Des., 155, June 2020
[45] J.L. Duchateau, et al., Conceptual design for the superconducting magnet system of a pulsed DEMO reactor, Fusion Eng. Des. 88 (2013), 1609-1612.
[46] C. Bachmann, DEMO Plant Requirements Document (PRD), EFDA_D_2MG7RD_v1.8, 2014
[47] R. Aymar, P. Barabaschi, Y. Shimomura, The ITER design, Plasma Physics and Controlled Fusion 44 (2002), 519.
[48] J. Harman, WP12 DEMO Operational Concept Description, EFDA_D_2LCY7A, 2012.
[49] A. Häußler, Computational approaches for nuclear design analyses of the stellarator power reactor HELIAS, DOI: 10.5445/IR/1000124072, https://publikationen.bibliothek.kit.edu/1000124072